

Supplementary Material

Sensitivity of excitatory LGMD input to the speed of object motion. Figure S1 below illustrates an experiment that demonstrates the sensitivity of local excitatory input to the LGMD to the speed of object motion. In these experiments, a small black disk (see Krapp and Hengstenberg, *Vis. Res.*, 1997, **37**:225-234 for details) was moved at various speeds close to the center of LGMD's receptive field and the dependence of the spiking response on speed was measured. The range of speeds tested covers the range expected for a looming object as it approaches the retina (between 72 and 1440 deg/sec; 1 cycle/sec = 360 deg/sec; see ref. 12, Fig. 1B). Activation of feedforward inhibition can be ruled out in these experiments due to the small object size. In contrast, lateral inhibition on the feedforward excitatory pathway could contribute to speed sensitivity. Figs. S2 and S3 below, plot the responses of the LGMD to simultaneous activation of several such local stimuli at various places in the cell's receptive field. The summation of responses elicited in the LGMD is sublinear; and therefore the 'size' of a moving object is not prominently represented in the excitatory pathway, at least postsynaptically.

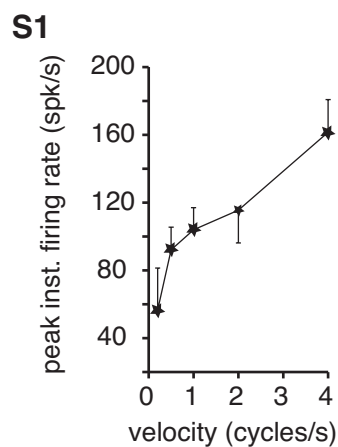
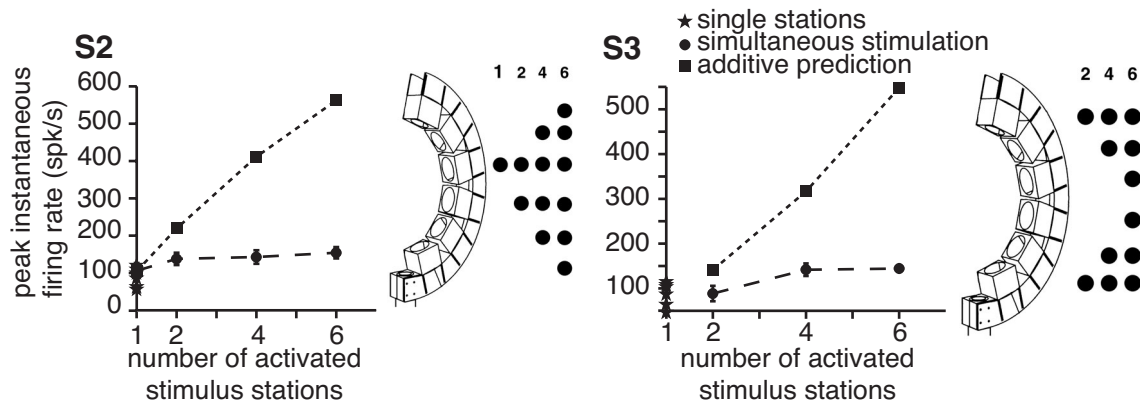


Fig. S1. The LGMD/DCMD was activated with a small disk moving at various speeds close to the center of the eye (abscissa, 1 cycle/sec = 360 deg/sec). The ordinate gives the peak instantaneous firing rate in response to such a stimulus (mean \pm sd over 5 repetitions; similar results were obtained when considering average number of spikes elicited in longer time windows).



Figs. S2, S3. Simultaneous activation of several small moving dots at different places in the receptive field of the LGMD/ DCMD. Insets on right show the position stimulated with a moving disk (up to 6 simultaneous stimuli, positioned on a single meridian and spaced 30 deg apart from -75 to +75 deg). Stars represent activation at a single location and dots simultaneous activation at various locations. Squares are linear prediction obtained from single station activation (stars). Note the strong sublinearity of the responses.

Fits of LGMD/DCMD firing rate to kinematical models. To fit the LGMD/DCMD firing rate, $f(t)$, we first performed linear regressions of the peak firing time relative to collision to determine the slope α and y-axis intercept δ of the best straight line fit to the data (see Fig. 1d, bottom; ref. 12). Three additional parameters that varied for each value of $l/|v|$ were the peak firing rate, f_{peak} , and two real power exponents, n_1 , n_2 , of a non-linearity x^n . Power exponents were separately fitted on the rising and decaying phase of the firing rate¹². If we define $x(t) = c_n \cdot \dot{\theta}(t - \delta)e^{-\alpha\theta(t-\delta)}$, where c_n is a constant normalizing the peak value of $x(t)$ to 1, the fit function is given by

$$f(t) = \begin{cases} f_{peak} x(t)^{n_1} & t \leq t_{peak}, \\ f_{peak} x(t)^{n_2} & t > t_{peak}. \end{cases} \quad (1)$$

Typical values were between 1.0 and 3.0 for n_1 and 0.1-2.0 for n_2 (in Fig. 1c, $f_{peak} = 128$ spk/s, $n_1 = 1.62$, $n_2 = 0.56$). See ref. 11 for fits on part of the $l/|v|$ range (5-25 ms) and ref. 12 for non-parametric fits on the whole range 5-50 ms. The additive models tested were based on two combinations of θ and $\dot{\theta}$: $[\dot{\theta} - \alpha\theta]$ and $[\dot{\theta} - \exp(\alpha\theta)]$, respectively. These two combinations could not fit the data, even when using a static non-linearity as above.

Satisfactory fits could only be obtained by compressing the angular velocity with respect to angular size, as in the combination $[\log \dot{\theta} - \alpha\theta]$ that corresponds to our multiplicative model (see main text).

Median filtering of membrane potential time-course. Median filtering used to extract the subthreshold membrane potential (Fig. 4) was performed with a 15ms sliding window (151 samples) centered on the considered membrane potential value. Identical results were obtained with windows twice or half as long. Median filtering of the membrane potential recorded at the spike initiation zone effectively eliminates the action potentials and permits the extraction of the underlying membrane potential envelope (Fig. 4a, b). The resulting voltage trace, \bar{v}_m , reflects both synaptic and subthreshold membrane conductance contributions. Comparison of the upper and lower panels in Fig. 4b suggests that subthreshold membrane conductances contribute significantly to \bar{v}_m . The activation of these subthreshold membrane conductances is TTX-sensitive, either directly or indirectly *via* spike generation mechanisms.

Table 1. Relation between firing rate ($\langle f \rangle$) and membrane potential ($\langle \bar{v}_m \rangle$).

This table reports statistical significance values of firing rate fits as a function of membrane potential (see Fig. 4d) for 3 different models (see Methods) during looming stimulus approach in 10 neurons. Values reported as single digits (0 or 1) are exact up to numerical resolution (double precision floating point); other values have been rounded beyond the last reported digit.

Experiment	power	linear	exponential	exp. only	power only
1.	1*	0	0.004		
2.	0.133*	0	0		
3.	1*	0	0		
4. ⁺	0.99*	0	0		
5.	0.092*	0	0		
6.	0.998*	0	0		
7.	1*	0	0.997*	0*	0.06
8.	0.25*	0.000	0.09*	0.001*	0.27
9.	1*	0	0.999*	0*	0.002*

Columns 2-4 are model lack of fit (F-test) from repeated trials. Lack of fit is always rejected (*, $p > 0.01$) for the power model, accepted for the linear model and rejected in expts. 7-9 for the exponential model. In those last 3 cases, we used a linear combination of power and exponential models to test whether one component may be set to 0 (last 2 columns). In all cases, the hypothesis of only an exponential term is rejected (*, $p < 0.01$) while only a power term is accepted in 7, 8. In expt. 9, both exponential and power terms cannot be ruled out.

^{||}One additional expt. could not be fitted with these 1-parameter models. ⁺Best fitted by 6th order power law.

Injection of PCTX and TTX in the lobula. Pipettes were micromanipulated and retracted immediately following drug injection to minimize diffusion in the bath. During extracellular recordings (PCTX injections) the pipette was positioned in physical contact with the lobula before injection. The effect of PCTX was immediate. Visual monitoring confirmed that only the lobula was reached by the injection. This makes it unlikely that the medulla or lamina neuropils (located several 100 μm away) were affected. During intracellular recordings the PCTX or TTX-injection pipette was positioned within 20 μm of the target site. Picospritzer output pressure was calibrated prior to the experiment by measuring ejected volumes in mineral oil. Ejected quantities were in the range of 2-20 nl. During TTX injections, the input resistance of the LGMD was routinely measured before and after drug injection. No changes were found and thus peak membrane voltage depolarizations observed after TTX injection were not caused by a partial inactivation of afferent excitation counterbalanced by an increase in postsynaptic input resistance.

Visual stimulation protocols. The fast optic flow stimulus was presented 200 ms and 150 ms prior to the last frame of looming stimulus expansion in the experiments described in Fig. 2 and 3, respectively. During extracellular recordings we used interstimulus presentation intervals (ISIs) of 3 min (total: 20 stimulus presentations or about 1 h) or 40 s (100 stimulus presentations or about 1 h 15 min). In 10 cases, animals were physically stimulated by gentle tapping of the dorsal cuticle between stimuli to minimize the effect of habituation. No differences in results were observed between these three protocols (see also Figs. 1 and 2 of ref. 12 and corresponding discussion). For intracellular recordings, interstimulus intervals were set at 20 s to compensate for shorter recording times and acquire sufficient data for statistical analyses. Shortened ISIs led to increased habituation in some experiments. During data analysis, we routinely screened for such effects.